Nonlinear dynamical modeling of compact toroids using the Fourier-Beltrami expansion

Preston Geren
Geren Consulting Services, Shoreline, WA

Loren Steinhauer
Redmond Plasma Physics Laboratory, University of Washington

Abstract

The nonlinear plasma dynamic equations can be converted to a set of ordinary differential equations in time using a Fourier-Beltrami expansion. Using a truncated basis set of the Beltrami vectors the dynamics can be computed. This unconventional model is used to explore the nonlinear stability of compact toroid plasmas. The angular momentum emerges as important ingredient in stability, although some poloidal flow appears to be necessary as well.

I. Introduction: Fourier-Beltrami analysis

A mystery about the stability of field-reversed configurations (FRC) persists after more than 25 years of investigation. In particular the ideal tilt mode is predicted to be unstable for all elongated, static FRC equilibria. Several stabilizing mechanisms have been investigated, notably two-fluid effects and finite Larmor radius (FLR). These are effective for small radius plasmas but not for reactor-relevant sizes. Moreover, a large part of the data base of stable FRC experiments lies outside the stable region predicted by the best theories. A recent possibility has been suggested by Belova [1] that nonlinear stability is achieved by a partly-tilted, dynamical state. Another possible stabilization mechanism suggested in recent years is sheared flow [2,3] methods for its analysis are not well developed. In short, stability remains *the* make-or-break issue for FRC as a fusion concept.

In this paper we focus on the possibility of flow stabilization. Here we apply an innovative method for its analysis, a Fourier expansion procedure. This method has been used in analyzing plasma turbulence but only recently was applied to ideal [4] and resistive [5] stability. This approach differs from familiar finite-difference (FD) methods in the way that the plasma structure is resolved. FD methods divide the plasma into a spatial grid whereas Fourier methods resolve the spatial structure into geometric modes.

The scale of the computational problem is similar for both methods, give a desired level of spatial resolution. However Fourier methods should give a clearer picture of mode-mode coupling effects. Further, $\nabla\cdot\mathbf{B} = 0$ can be made automatic with a Fourier expansion (for proper choice of basis set) whereas the imperfect satisfaction of this equation remains an issue with FD methods.

The Fourier method adopted here is the Fourier-Beltrami (FB) expansion procedure by which the fields and flows are expanded in Beltrami vectors. The Beltrami vectors satisfy $\nabla\times\mathbf{Y}_k = \Lambda_k\mathbf{Y}_k$ with suitable B.C.; Λ_k is the eigenvalue, and k is the index. The $\{\mathbf{Y}_k\}$ is a complete basis set for all divergence-free vectors. If then an incompressible plasma is assumed (uniform density so that $\nabla\cdot\mathbf{u}$

= 0) then the Beltrami vectors serve as a complete basis set for both the field $\mathbf{B}(\mathbf{r},t)$ and flow $\mathbf{u}(\mathbf{r},t)$. These are expanded as $\mathbf{B} = \Sigma B_k(t)\mathbf{Y}_k(\mathbf{r})$, $\mathbf{u} = \Sigma u_k(t)\mathbf{Y}_k(\mathbf{r})$. The vector equations (motion, Maxwell's) are then converted into a system of coupled ordinary differential equations in time. The equation of motion is

$$\frac{d}{dt}u_k \quad = \quad -\Pr\frac{\eta c^2}{4\pi}\Lambda_k^2 u_k + \sum_{l,m} M_{klm}\left(\Lambda_m u_l u_m + \Lambda_l \frac{B_l B_m}{4\pi m_i n}\right) \qquad (1)$$

where the terms on the right side are, successively, the viscous friction, convective inertia, and $\mathbf{j}\times\mathbf{B}$ force. The generalized Ohm's law is

$$\frac{d}{dt}B_k \quad = \quad -\frac{\eta c^2}{4\pi}\Lambda_k^2 B_k + \sum_{l,m}\left(u_l - \ell_i^2 \frac{e}{m_i c}\Lambda_l B_l\right) M_{klm}\Lambda_k B_m \qquad (2)$$

The terms are electric field (LHS), resistive friction, $\mathbf{u}\times\mathbf{B}$ term, and Hall effect. The ℓ_i is the ion skin depth. In the discussion that follows the time evolution of the various B_k, u_k will be examined. These are referred to as "modes" although they are not the familiar normal modes of linear stability theory. The M_{klm} in these equations are the triple scalar products linking the various modes; they have three indices because they link three modes in the manner of a three-wave interation. These give rise to nonlinear mode-mode coupling.

II. Role of angular momentum: clues from minimum energy theory

The importance of angular momentum emerges from the theory of minimum energy states (MES). The two-fluid minimum-energy theory minimizes the magnetofluid energy $W_{mf} \sim \int d^3x(B^2+u^2)$ subject to constraints on the global ideal invariants of the system. For a two fluid these are the helicities for the electrons and ions, $K_e \sim \int d^3x \mathbf{A}\cdot\nabla\times\mathbf{A}$ and $K_i \sim \int \mathrm{d}^3\mathrm{x}(\mathbf{A}+\mathbf{u})\cdot\nabla\times(\mathbf{A}+\mathbf{u})$, respectively. Also, if the domain is axisymmetric and there is a free-slip condition at the boundary, then angular momentum is conserved as well. Although angular momentum conservation was accounted for in the original minimum-energy work of Woltjer [6], it has largely been ignored since then.

The critical role of angular momentum in affecting the state of minimum energy was only recently uncovered [7]. Given the invariants $\{K_e,K_i\}$ the states of stationary energy, found by using the method of Lagrange multipliers, is composed of two elements. solving the is composed of two elements; using the Beltrami vectors these are $\mathbf{B} = B_1\mathbf{Y}_1 + B_2\mathbf{Y}_2$, $\mathbf{u} = u_1\mathbf{Y}_1 + u_2\mathbf{Y}_2$ associated with the two eigenvalues, Λ_1 and Λ_2. It was shown [7] that for *the* MES, one of the eigenvalues, is large, $\Lambda_2 \to \infty$. Even a small dissipation would damp the fine-scale element, leaving behind a force-free plasma (Taylor state). However, if angular momentum is included among the constraints $\{K_e,K_i,L_z\}$ then the MES is modified. If the angular momentum is comparable to that associated with diamagnetic drift, then the MES is smooth, i.e. its length scales are comparable to the domain size. This suggests, although it doesn't prove, that angular momentum is an important ingredient in the stability of flowing plasmas.

III. Truncated basis set for nonlinear plasma dynamics

A convenient domain geometry to use is the periodic-cylinder (P-C) because analytic forms are available for the Beltrami vectors [8]. This domain is useful for compact toroids of arbitrary elongation. Unfortunately the P-C has an important defect with respect to the problem at hand: the full periodic cell length is composed of two compact toroid "cells" as shown in Fig. 1. The internal "surfaces" are

indicative of the poloidal structure of the lowest-order Beltrami vector. The angular momentum of the two cells is opposite so that the total angular momentum is zero. It is intended that the angular momentum of a single cell be constant. This is not so in general. However, for certain choices of the basis set, the angular momentum of a single cell may be preserved *roughly*. In these cases the choice of basis set may restore the actual stabilizing effect of conserved angular momentum. On the other hand, the use of a limited basis set is always fraught with danger and may lead to apparent stability that will disappear with a more complete basis set. All that can be said is that the appearance of stability when angular momentum is preserved is an indicator of its stabilizing effect.

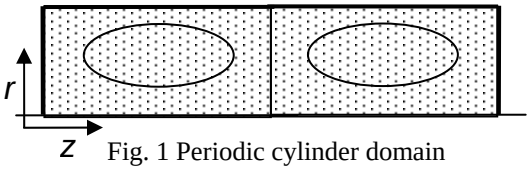

Fig. 1 Periodic cylinder domain

IV. Computational results with "8-pack"

Computations of the dynamical equations (1,2) have been performed for basis sets from 6 ("six-pack") to 60 ("60-pack") basis vectors. Attention is focused here on the 8-pack which in many cases roughly preserves the angular momentum. The elements of the 8-pack are shown in Fig. 2. For each of the forms there are elements with both positive and negative eigenvalues with the same magnitude. This makes a total of four axi-symmetric basis elements ($\mathbf{Y}_1$, $\mathbf{Y}_2$, $\mathbf{Y}_3$, $\mathbf{Y}_4$) and four non-axi-symmetric basis elements ($\mathbf{Y}_5$, $\mathbf{Y}_6$, $\mathbf{Y}_7$, $\mathbf{Y}_8$).

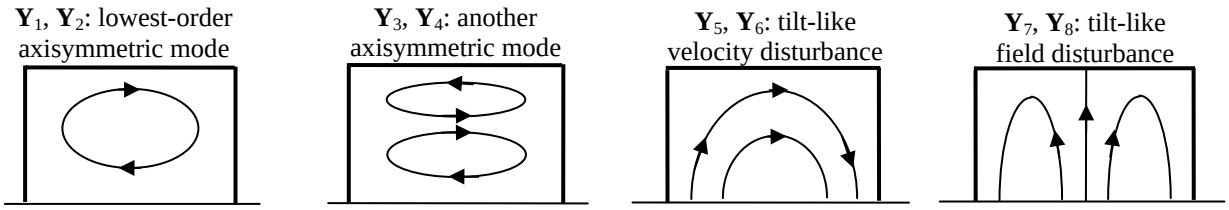

Fig. 2. Elements of the 8-pack

A. Tilt mode in a static FRC. As a baseline check the stability of the tilt mode in a static FRC is computed. In the static FRC the only nonzero axisymmetric coefficients, initially, are $B_1 = B_2 = 0.7$. A 1% initial disturbance is given to the non-axisymmetric velocity elements $u_5 = u_6 = u_7 = u_8 = 0.01$; the initial non-axisymmetric field elements are zero. The results of the tilt velocity are shown in Fig. 3. The linear growth rate of the tilt mode is $\gamma = 1.06V_A/b$ where V_A is the Alfven speed for the reference magnetic field (at midplane on the axis) and b is the half-length of the single-cell FRC. This result is consistent with linear theory. After an initial 1% disturbance, nonlinearity is reached after about two tilt growth times. The history of the angular momentum in Fig. 4. Here Ω is the average angular velocity and $S_* = a$ = domain radius ÷ ion skin depth. The angular momentum is conserved only during the linear growth period.

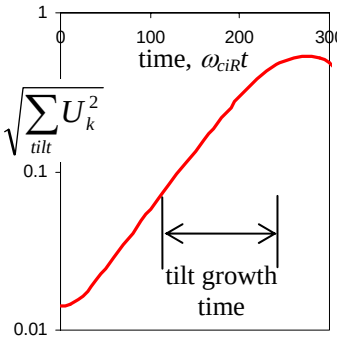

Fig. 3. Growth of tilt velocity disturbance

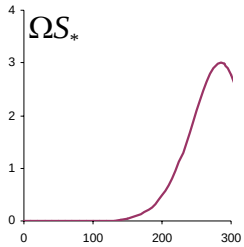

Fig. 4. Angular momentum history

Another way to portray the nonlinear tilt is by a phase plane plot, u_k vs B_k for the modes. Figures 5,6 show the trajectories of the axi- and non-axi-symmetric modes respectively. The black circle locates the

startining point for the initially non-zero coefficients. Large, persistent, and irregular oscillations are apparent. There is no resistive or viscous damping in these computations so that the trajectories do not approach a limit cycle.

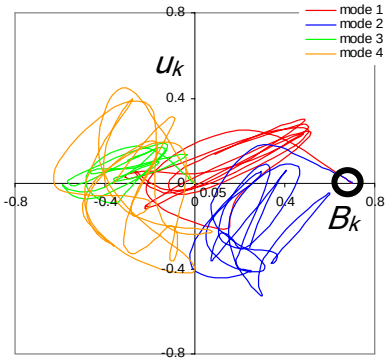

Fig. 5. Axi-symmetric modes

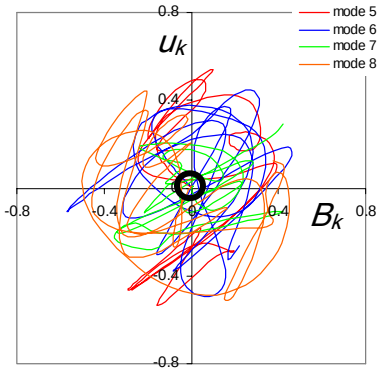

Fig. 6. non-axi-symmetric modes

B. Unstable example with poloidal flow. Figures 7,8 show an example with significant poloidal flow an (also) no initial angular momentum. Here the initial nonzero mode coefficients are $B_1 = 0.7$, $B_2 = 0.545$, $u_1 = u_2 = -0.4$, $u_5 = u_6 = u_7 = u_8 = 0.1$. This example is has $K_i = 0$, $K_e = 1$, and zero initial angular momentum, but in the dynamical evolution, it is not conserved. Thus the instability of the intial state may be exaggerated.

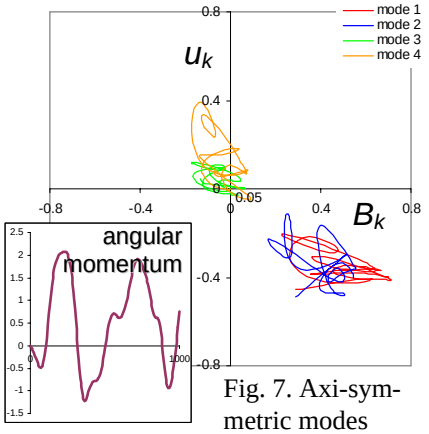

Fig. 7. Axi-symmetric modes

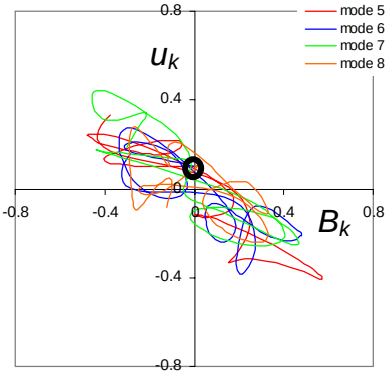

Fig. 8. Non-axi-symmetric modes

C. Stable example with poloidal flow. Consider the same case as in Figs. 7,8 but with initial angular momentum: $B_1 = 0.7$, $B_2 = 0.545$, $u_1 = -0.5502$, $u_2 = -0.2498$, $u_5 = u_6 = u_7 = u_8 = 0.1$. This example also has $K_i = 0$, $K_e = 1$, but angular momentum $\Omega S_* = -4$. The dynamical trajectories are shown in Figs. 9,10. Here the plasma is stable with well-bounded perturbations.

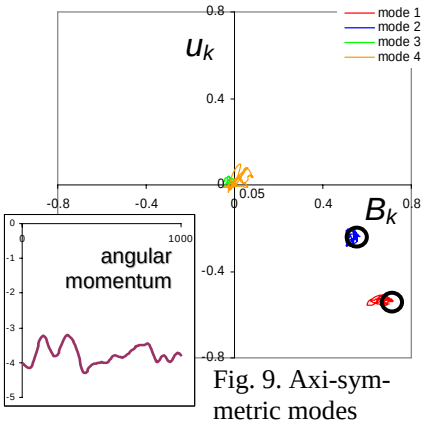

Fig. 9. Axi-symmetric modes

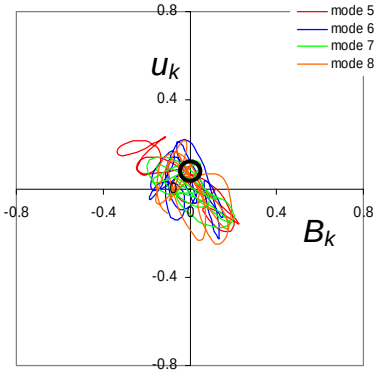

Fig. 10. Non-axi-symmetric

Note that the angular momentum is roughly conserved. Figures 11,12 show the poloidal field structure and the field structure at the midplane, respectively (axisymmetric field elements). Mean fields are shown over the time interval 100 to 1000 dimensionless time units. The configuration is a "near" FRC with a modest azimuthal field.

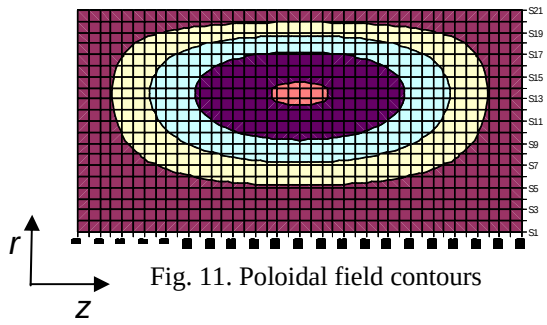

Fig. 11. Poloidal field contours

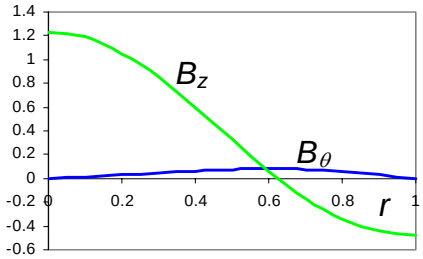

Fig. 12. Radial structure at midplane

The 8-pack has the property that it roughly preserves the angular momentum in some cases. In general though a basis set will not. This is illustrated in Figs. 13 where the trajectories for a 60-pack are shown for the same initial conditions as in Figs. 9-12. The same modes as in the earlier figures are shown although they are numbered differently in the 60-pack. Compare the axi-symmetric mode trajectories for the 60-pack in Fig. 13 with those for the 8-pack in Fig. 9. Evidently the angular momentum is not preserved in the 60-pack, and the behavior is unstable. What is not know is whether the apparent stability of the 8-pack is a physical consequence of the angular momentum conservation or an unphysical consequence of the limited basis set.

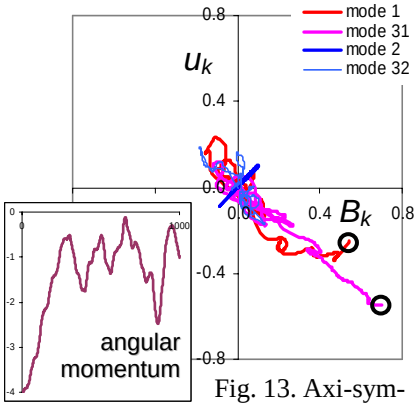

Fig. 13. Axi-symmetric modes

D. Stability parameter study. Consider a series of equilibria where only one parameter is varied. Use the same initial conditions as in Secs. IV-B,C except for varying u_1,u_2. If the sum $u_1 + u_2$ is fixed at –0.8 but the difference between the two is varied, then the poloidal flow is kept the same but the rotation ΩS_* (hence angular momentum) is varied. The stability is represented in terms of the averaged values of the magnetic field for both axisymmetric and non-axisymmetric modes. The results are shown in Fig. 14. For rotation ΩS_* less than about –4 the behavior is stable, i.e. the non-axisymmetric mean fields $\overline{B} \equiv \sqrt{\sum B_k^2}$ and "fluctuations" $\Delta B \equiv \sqrt{\sum \left(B_k - \overline{B}\right)^2}$ are relatively small for the non-axisymmetric modes. The "smallness" is only relative since the computations assume no dissipation so that suppressed modes oscillate at a relatively low amplitude rather than damping. However, for rotation ΩS_* exceeding about –4, the non-axisymmetric field becomes comparable to the axisymmetric field, indicating persistent unstable behavior. Note that negative rotation (required for stability) is in the direction of the ion diamagnetic drift.

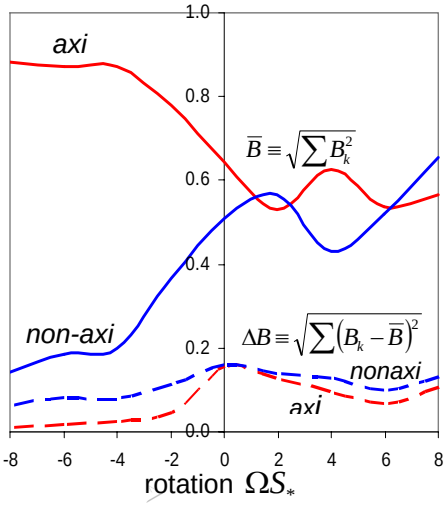

Fig. 14. Stability of a series of equilibria

Not shown in Fig. 14 is an index of how well the angular momentum is preserved. It is roughly constant in the stable regime but is not preserved in the unstable regime. Thus the instability may be exaggerated.

V. Conclusions

The results presented here strengthen the connection between angular momentum and stability. Hints to this fact originally appeared in analysis of minimum energy states, and appear to carry over to time-dependent plasmas as well. The main caveat that must be kept in mind is that these results are for a very limited basis set of eight vectors. Further, the complete basis set, Beltrami functions for a periodic-cylinder, are set up in such a way that angular momentum conservation does not necessarily play a role. However, for certain truncated basis sets and certain initial conditions, the angular momentum of a "single-cell" compact toroid is roughly preserved. In these cases apparent stability is achieved for certain conditions depending on the angular momentum. The key question is then whether this stability is (a) the consequence of taking to small a basis set and therefore excluding dynamics that would actually lead to instability, or (b) the consequence of angular momentum conservation. If the former, then the results here are unphysical, simply a feature of the incomplete mathematical model. If the latter, then the prediction of stability is an actual, physical result. To resolve this question will require the construction of Beltrami vectors for a domain where angular momentum conservation of a "single-cell" compact toroid is guaranteed. An example of such a domain is the "cylindrical can" investigated in a limited way some years ago [9,10].

References

[1] E.V. Belova, R.C. Davidson, Hantao Ji, and M. Yamada, Phys. Plasmas **11**,2523 (2004).

[2] L. C. Steinhauer and A. Ishida, Phys. Rev. Lett. **79**, 3423 (1997).

[3] L. C. Steinhauer and A. Ishida, Phys. Plasmas **5**, 2609 (1998).

[4] E.C. Morse, Phys. Plasmas **5**, 1354 (1998).

[5] E.C. Morse, D.D. Hua, and T.K. Fowler, International Sherwood Fusion Theory Conference, Santa Fe, 2-4 April 2001.

[6] L. Woltjer, Proc. Nat. Acad. Sci. **44**, 833 (1958).

[7] P. Geren and L.C. Steinhauer, Phys. Plasmas **11**, 3646 (2004).

[8] L. Turner, Nucl. Instr. Meth. **207**, 23 (1983).

[9] J.M. Finn, W. Manheimer, and E. Ott. Phys. Fluids **24**, 1336 (1981).

[10] L. Turner, Phys. Fluids **27**, 1677 (1984).